Direct Synthesis of Bifunctionalized Hexagonal Mesoporous Silicas and Its Catalytic Performance for Aerobic Oxidation of Cyclohexane

ARTICLE *in* THE JOURNAL OF PHYSICAL CHEMISTRY C · FEBRUARY 2009

Impact Factor: 4.77 · DOI: 10.1021/jp809427t

6 AUTHORS, INCLUDING:

Chen Chen
Van Andel Research Institute
59 PUBLICATIONS **756** CITATIONS
SEE PROFILE

Hong Ma
Chinese Academy of Sciences
43 PUBLICATIONS **602** CITATIONS
SEE PROFILE

Direct Synthesis of Bifunctionalized Hexagonal Mesoporous Silicas and Its Catalytic Performance for Aerobic Oxidation of Cyclohexane

Chen Chen, Jie Xu,* Qiaohong Zhang, Hong Ma, Hong Miao, and Lipeng Zhou

State Key Laboratory of Catalysis, Dalian Institute of Chemical Physics, Chinese Academy of Sciences, 457 Zhongshan Road, Dalian, P. R. China 116023

Received: October 24, 2008; Revised Manuscript Received: November 26, 2008

According to the characteristics of the cyclohexane oxidation reaction a series of bifunctionalized hexagonal mesoporous silicas, CoPh-HMS, were designed and successfully synthesized by a one-step co-condensation route. The results of small-angle XRD, TEM, and N_2 adsorption−desorption measurements showed that the resultant materials had well-ordered mesoscopic structures. Co^{2+} ions were incorporated into the frameworks in tetrahedral coordination along with phenyl groups immobilized on the surface, confirmed by a careful spectroscopic (FT-IR, UV−visible, and ^{29}Si MAS NMR) study. The surfaces of the materials were proved to be more hydrophobic with higher Ph loading, and the largest water droplet contact angle is up to 110.50°. These materials were applied in the liquid-phase oxidation of cyclohexane with molecular oxygen as oxidant and *tert*-butyl hydroperoxide as initiator under solvent-free conditions. High activity could be obtained with these bifunctionalized catalysts being used. The modification effect of phenyl groups played an important role in the activity enhancement.

1. Introduction

Apart from its intrinsic importance in the chemistry of C−H activation selective oxidation of cyclohexane to yield cyclohexanone and cyclohexanol (the so-called K−A oil) is the centerpiece of the commercial production of Nylon. More than 10^6 tones of cyclohexanone and cyclohexanol are produced worldwide per annum.[1] In practice, oxidation of cyclohexane is carried out at 423−433 K without catalyst or with a homogeneous catalyst. Since cyclohexanone and cyclohexanol are substantially more reactive than the cyclohexane reactant and easily further oxidized to deep-oxidation products, high (80%) selectivity to K−A oil is obtained only at low (<5%) cyclohexane conversion.[2] For these reasons, many attempts have been made to substitute the traditional process by developing heterogeneous catalysts with molecular oxygen in the absence of solvent. Under these conditions, FeCoMnAPO-5 gave 6.8% cyclohexane conversion and 65.1% selectivity to K−A oil.[3] MnAPO-36 was found to be the most active catalyst, and 13% cyclohexane conversion with 62% selectivity to K−A oil were obtained at 403 K for 24 h under 1.5 MPa air pressure.[4] On the whole, most of these systems showed relatively low selectivity to the desired products (K−A oil) or exhibited low activity. As Schuchardt acknowledged, although many attempts have been made in the cyclohexane oxidation, it continues to be a challenge.[5]

In the oxidation reaction of cyclohexane the substrate is a nonpolar molecule while the oxygenated products are polar molecules. According to these characteristics an efficient catalyst may be designed by encompassing two elementary factors: first, it has catalytically active sites; second, its surface should be hydrophobic, which facilitates adsorption of nonpolar cyclohexane and desorption of the polar oxygenated products, resulting in high conversion and selectivity. A method for potentially accomplishing this goal would be incorporation of metal ions and introduction of hydrophobic organic groups into the catalyst. The hexagonal mesoporous silica (HMS) is such a proper candidate to be modified, which possesses wormhole-like or sponge-like framework structures, large surface area, and narrow pore size distribution.[6] Compared with the other kinds of mesoporous siliceous material possessing long-range hexagonal framework structures, HMS has further advantages: HMS possesses thicker framework walls, smaller crystallite size of primary particles with shorter channels, and larger textual mesoporosity, which may provide better transport channels for reactants to the active sites and better diffusion channels for products to move out.[7] These properties enable HMS attractive for application in catalysis. Usually there are two approaches for functionalization of HMS: one is incorporation of transition metals into the frameworks;[8−12] the other is surface modification with organic groups.[13,14] We can simultaneously utilize these two approaches to realize our design: the former is utilized to create catalytically active sites, and the latter is utilized to change the physical properties of the materials (e.g., their hydrophobicity and adsorption characteristics). Introduction of hydrophobic groups into the mesopores can create a hydrophobic environment that will continuously exclude K−A oil from the mesopores and absorb cyclohexane into the mesopores. Conversion of cyclohexane can be facilitated, while further transformations of K−A oil can be inhibited, so the goal to increase conversion and selectivity for K−A oil may be accomplished. This was preliminarily realized,[15] and the inherent causes were systematically studied in the present work.

2. Experimental Section

2.1. Synthesis. Tetraethyl orthosilicate (TEOS, $Si(OEt)_4$, 99%), cobaltous acetate ($Co(OAc)_2 \cdot 4H_2O$, 99%), ethanol (C_2H_5OH, 99.5%), ammonium nitrate (NH_4NO_3, 99.0%), and mesitylene (C_9H_{12}, 98%) were obtained from Tianjin Kermel Chemical Reagent Development Center, China. Hexadecylamine (HDA, $C_{16}H_{35}N$, 90%) was obtained from Alfa Aesar. Phenyltriethoxysilanes (PTES, 99%) was obtained from Aldrich.

* To whom correspondence should be addressed. Phone: 86-411-84379245. Fax: 86-411-84379245. E-mail: xujie@dicp.ac.cn.

10.1021/jp809427t CCC: $40.75
Published on Web 01/26/2009

The bifunctionalized materials were synthesized from the gels with the following molar composition: 0.02Co:(1 − *x*) TEOS: *x*PTES:0.27HDA:0.27mesitylene:9C_2H_5OH:72H_2O, where x = 0.1, 0.2, 0.3, and 0.4. In a typical synthesis the calculated amounts of ethanol, deionized water, and hexadecylamine were stirred for 20 min at room temperature. To this gel, solution A (TEO (8.32 g) and PTES (2.40 g)) and solution B ($Co(OAc)_2 \cdot 4H_2O$ (0.25 g) and deionized water (10 g)) were simultaneously added very slowly under vigorous stirring. After 5 min mesitylene (1.62 g) was added as swelling agent. Stirring was continued for 24 h. It was then filtered, washed with deionized water, and dried at 353 K for 12 h. The template was removed from the as-synthesized material by NH_4NO_3/ethanol extraction. A 1.0 g amount of sample was stirred in a mixture of ethanol (100 mL) and NH_4NO_3 aqueous solution (6 wt %, 5.3 g) for 15 min at 351 K. The solid was recovered by filtration and repeatedly washed with an excess of ethanol. The process was then repeated until the template was removed completely. The material was further dried at 353 K for 12 h.[15] The samples synthesized by this method are designated as CoPh-HMS-xx, where xx are mol % of PTES of total Si in the gels. A pure siliceous HMS was synthesized without $Co(OAc)_2$, PTES, and mesitylene. Nonorganofunctionalized Co-HMS was synthesized without PTES and mesitylene.

2.2. Characterization. X-ray powder diffraction (XRD) patterns were obtained using a Rigaku D/Max 3400 powder diffraction system with Cu Kα radiation (λ = 0.1542 nm). Fourier transform infrared (FT-IR) spectra were collected between 4000 and 400 cm^{-1} on a Bruker Tensor 27 FT-IR spectrometer in KBr media. The surface area and pore volume was determined by N_2 adsorption−desorption measurement at 77 K on an ASAP 2010 micromeritics instrument. The samples were degassed at 353 K for 24 h prior to the adsorption measurements. Ultraviolet−visible diffuse reflectance spectra (UV−vis DRS) were collected over a wavelength range from 800 to 200 nm on a Jasco V-550 UV−vis spectrophotometer equipped with a diffuse reflectance attachment. The microstructures of the materials were examined by transmission electron microscopy (TEM) on a JEOL JEM-2000EX electron microscope at an accelerating voltage of 120 kV. The nuclear magnetic resonance spectra of ^{29}Si with magic-angle spinning (^{29}Si MAS NMR) were taken on a Bruker DRX-400 spectrometer at 79.5 MHz with a spinning frequency of 4 kHz. Before evaluating the hydrophobicity the materials were first pressed into flakes under 6 MPa; then the contact angles formed between sessile water droplets and the flakes were measured using a contact angle measuring system JC 2000A.

2.3. Catalytic Oxidation of Cyclohexane. Catalytic reactions were performed in a 100 mL autoclave reactor with a Teflon insert inside. Typically, 15.00 g of cyclohexane, 0.12 g of *tert*-butyl hydroperoxide (TBHP, 65 wt %), and 0.12 g of catalyst were placed in the reactor. Then, after sealing, the reactor was heated to the reaction temperature, while agitation was ensured by an external magnetic stirrer. Upon heating to the reaction temperature the reactor was charged with 1.0 MPa of O_2 and O_2 was fed continuously to maintain constant pressure. When the reaction stopped the catalyst was separated by filtration after the reaction mixture was diluted with 15.00 g of ethanol to dissolve the byproduct. The reaction products were identified by an Agilent 6890N GC/5973 MS detector and quantitated by an Agilent 4890D GC equipped with a OV-1701 column (30 m × 0.25 mm × 0.3 μm) and titration. After decomposition of CHHP to cyclohexanol by adding triphenylphosphine to the reaction mixture, cyclohexanone and cyclohexanol were determined by the internal standard method using methylbenzene as an internal standard. The concentration of CHHP was determined by iodometric titration and the byproduct acid and ester by acid−base titration.[15] The mass balance in our experiment is above 92%.

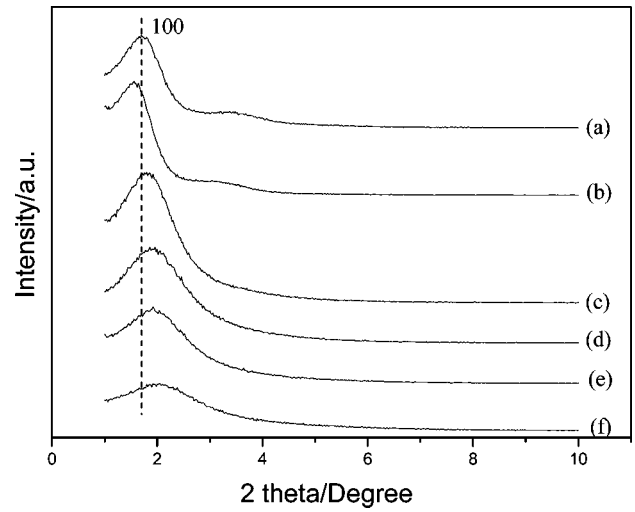

Figure 1. Small-angle XRD patterns of (a) HMS, (b) Co-HMS, and CoPh-HMS-xx (where xx = (c) 10, (d) 20, (e) 30, and (f) 40).

TABLE 1: Textural Parameters of HMS, Co-HMS, and CoPh-HMS-xx (where xx = 10, 20, 30, and 40)

sample	d_{100} (nm)	a_0[a] (nm)	pore size[b] (nm)	surface area[c] (m^2/g)	pore volume[b] (mL/g)
HMS	5.2	6.0	5.2	670	0.90
Co-HMS	5.4	6.2	4.4	682	0.72
CoPh-HMS-10	4.8	5.6	3.4	942	0.84
CoPh-HMS-20	4.6	5.3	2.7	899	0.52
CoPh-HMS-30	4.5	5.2	2.7	742	0.35
CoPh-HMS-40	4.3	5.0	2.7	481	0.19

[a] $a_0 = 2d_{100}/\sqrt{3}$. [b] Calculated from the desorption branch of the nitrogen adsorption and desorption isotherms using the BJH model. [c] The BET method was used to calculate the surface area.

3. Results and Discussion

The small-angle X-ray diffraction patterns of HMS, Co-HMS, and CoPh-HMS-xx are shown in Figure 1. All samples exhibit the diffraction peak corresponding to the (100) plane at 2θ of 1−4°. Materials exhibiting this single low-angle peak are considered to possess short-range hexagonal symmetry with uniform pore diameter.[6] At comparatively lower PTES content (≤20 mol %) the d_{100} diffraction peaks of the materials are intensive. These phenomena suggest cobalt incorporation and phenyl immobilization did not change the mesoporous structure. While the content of PTES in the starting gel reaches 40 mol %, the evident decrease in XRD peak intensity is observed, meaning that the mesoporous structure was partly destroyed with superabundant Ph loading. Compared with that of the pure silica HMS, the d_{100} diffraction peak of Co-HMS shifts toward the lower angle. This suggests that the d spacing and unit cell parameter of Co-HMS is bigger than that of its pure silica analogue (Table 1). The above results imply that cobalt has been incorporated into the framework of HMS for the radius of Co^{2+} (0.074 nm) is larger than the radius of Si^{4+} (0.026 nm). This situation is similar to HMS containing tin, vanadium, and iron.[10,11] In addition, for the bifunctionalized materials a shift to higher angle is observed at higher Ph loading, indicating contraction of the lattice with phenyl immobilization on the

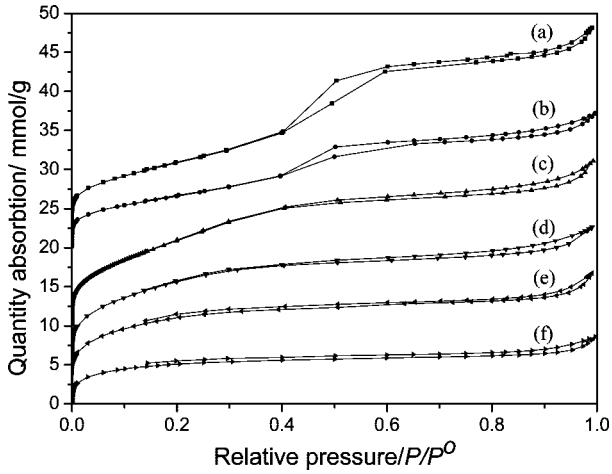

Figure 2. N_2 adsorption−desorption isotherms of (a) HMS, (b) Co-HMS, and CoPh-HMS-xx (where xx = (c) 10, (d) 20, (e) 30, and (f) 40).

surface. It is known that a neutral templating mechanism (S^0I^0) was followed to synthesize HMS that is based on hydrogen bonding and self-assembly between neutral primary amine surfactant (S^0) and neutral inorganic precursor (I^0).[6] Similar to the finding of Lim and co-workers,[16] the surfactant−silicate interface, in which the phenyl groups might be located, becomes a balanceable region between S^0 and I^0 due to the effect of hydrogen bonding and self-assembly. With the increase of PTES concentrations the density of silanol groups in this interface decreases and fewer surfactant molecules are required for balance. This situation leads to contraction of the micelle size in the bifunctionalized mesoporous materials with higher concentrations of PTES.

Figure 2 shows the N_2 adsorption−desorption isotherms of HMS, Co-HMS, and CoPh-HMS-xx. All materials show type IV isotherms with hysteresis loops as defined by IUPAC for mesoporous materials and therefore are mesoporous materials, although the presence of micropores can be detected at lower relative pressure. At a lower content of PTES (≤20 mol %) the isotherms of the materials exhibit the sharp inflection characteristic of capillary condensation within the uniform mesopores. However, at higher content of PTES (≥30 mol %) the hysteresis loops broaden and exhibit H4-type behavior, indicating greater disorder occurred and a decrease of mesoporosity caused by higher Ph loading. Wahab and co-workers observed a similar phenomenon for hybrid periodic mesoporous organosilica materials.[17] Table 1 lists the detailed structural parameters of all the mesoporous materials. The decrease in surface area, pore volume, and pore size imply reductions in the free channel space as more phenyl groups were immobilized on the surface of the channels.

Transmission electron microscopy (TEM) images of all samples show that the materials synthesized in our work possess the typical wormhole structures of HMS material assembled from long alkyl chain neutral amines as template (Figure 3).[18] Consistent with the results of N_2 adsorption−desorption measurements (Table 1), the pore dimension is found to be reduced after organofunctionalization caused by immobilization of phenyl groups on the inner surface of the pores. Besides, analogous images are observed for HMS, CoHMS, and CoPh-HMS-xx, indicating that cobalt species and phenyl groups are highly dispersed or imbedded in the silica matrix. It can also be observed that, compared with the other samples, CoPh-HMS-40 possesses the worse mesoporosity. This is consistent with the results of XRD.

In order to study the coordination geometry of cobalt incorporated in the materials, UV−vis DRS were detected (Figure 4). The spectra of all the samples display three absorption peaks at around 525, 584, and 650 nm. The triplet peak is characteristic for tetrahedral Co^{2+} and due to the $^4A_2(F) \rightarrow {}^4T_1(P)$ energy transition.[19,20] The absence of peaks at ca. 480 and 506 nm indicates the absence of Co^{2+} in an octahedral environment,[21] and the absence of peaks at 356 and 410 nm indicates the absence of Co^{3+}.[22] These results reveal that the majority of the Co^{2+} ions in the samples occupy framework positions of the channel walls.[19,20,23] Moreover, in the spectra of CoPh-HMS-xx two intense bands in the UV region centered at 212 and 262 nm exhibiting characteristic vibrational structure are observed. These absorption bands are assigned to π–π^* transitions of benzene ring.[24] The emergence of these two bands can be taken as strong evidence for successful immobilization of phenyl groups on these bifunctionalized materials.

Figure 5 shows the infrared spectra of these samples. Typical bands associated with formation of a condensed siloxane network were present in all cases (Si−O−Si bands around 1228, 1070, 798, and 465 cm^{-1}).[25] As reported in the literature, solvent extraction could be utilized to remove the template molecules.[15] The corresponding bands about the template molecules almost disappeared for all samples, indicating the organic template was removed. Typical bands associated with =CH stretching aromatic vibrations (weak peaks around 3030−3080 cm^{-1}) with Si−Ph vibrations (around 1137, 740, and 698 cm^{-1}) and phenyl ring vibrations (weak peaks at 1600 and 1437 cm^{-1}) were detected in all spectra of CoPh-HMS-xx.[26] These bands indicate that phenyl groups were introduced in the CoPh-HMS-xx samples. This is also consistent with the UV−vis DRS. The intensity of these absorption bands increases with Ph-loading increase. The absorption band around 465 cm^{-1} is assigned to O−Si−O bending vibration.[27] Phenyl immobilizations cause the monotonic blue shift of this band to higher wave numbers. This may be caused by the partial substitution of Si−O with Si−Ph, and the bending vibration of O−Si−O is affected by the neighboring phenyl groups. Therefore, this result may be considered as supplementary proof of successful immobilization of phenyl groups in CoPh-HMS-xx. In addition, the absorption band at 960 cm^{-1} was assigned to Si−O stretching in the Si−OH group in mesoporous siliceous material.[28] The intensity of these bands decrease with Ph-loading increase, which should be due to the decrease of the amount of Si−OH on the surface caused by substitution with Si−Ph. In the spectrum of CoPh-HMS-40 this band can hardly be identified, indicating few Si−OH existing on the surface of the material, and the surface should turn hydrophobic owing to immobilization of hydrophobic phenyl groups.

The ^{29}Si MAS NMR spectra of these materials are shown in Figure 6. For the spectrum of Co-HMS it shows characteristic peaks at around −102 and −110 ppm, which are assigned to Q^3 and Q^4 species, respectively.[29] After functionalization with organic groups, besides these two peaks, resonances characterizing the organosiloxane network [T^m=$RSi(OSi)_m(OH)_{3-m}$, m = 1−3] are observed in all spectra of CoPh-HMS-xx.[29,30] The appearance of organosilane signals between −70 and −90 ppm (T^3 = $PhSi(OSi)_3$ and T^2 = $PhSi(OSi)_2(OH)$) are characteristics of fully cross-linked organosiloxane species. Moreover, the ratios of Q^3 ($Si(OSi)_3(OH)$) silicate to total silicon in the spectra of CoPh-HMS-xx decrease, while the ratios of T^3 to total silicon increase with Ph-loading increase. These results indicate that the amount of Si−OH decreases with replacement of Si−OH by more Si−Ph on the surface of these bifunctionalized

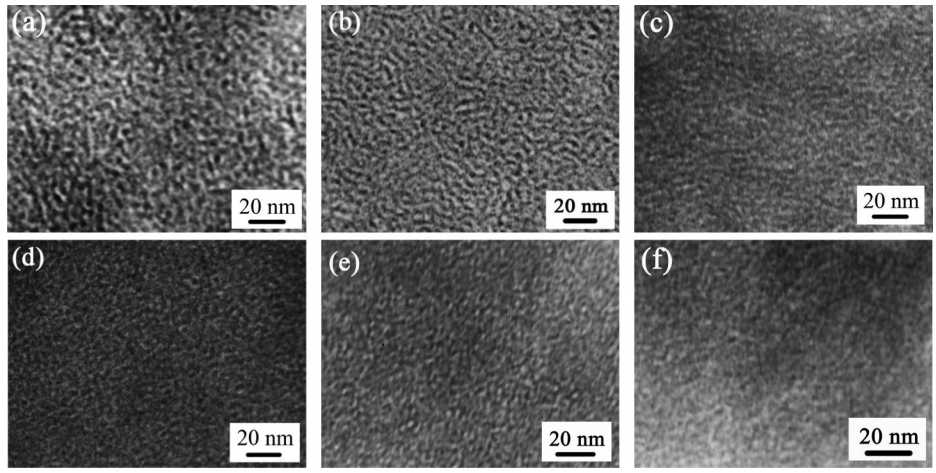

Figure 3. TEM images of (a) HMS, (b) Co-HMS, and CoPh-HMS-xx (where xx = (c) 10, (d) 20, (e) 30, and (f) 40).

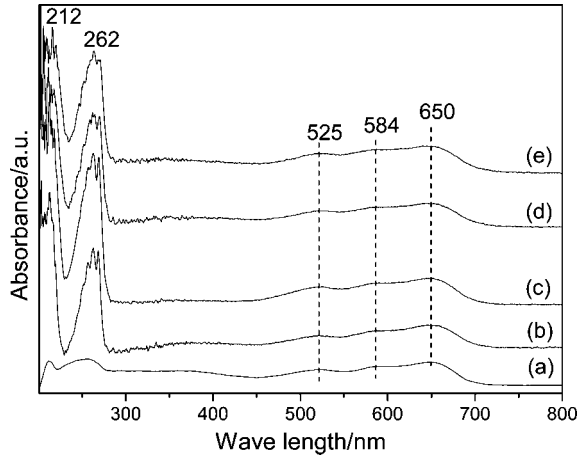

Figure 4. UV−vis DRS of (a) Co-HMS and CoPh-HMS-xx (where xx = (b) 10, (c) 20, (d) 30, and (e) 40).

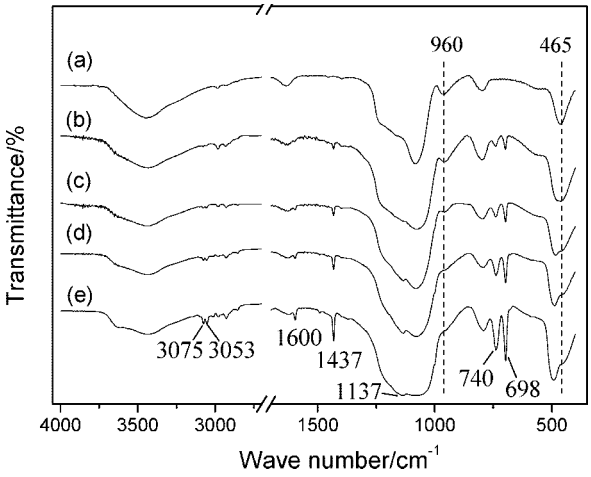

Figure 5. FT-IR spectra of (a) Co-HMS and CoPh-HMS-xx (where xx = (b) 10, (c) 20, (d) 30, and (e) 40).

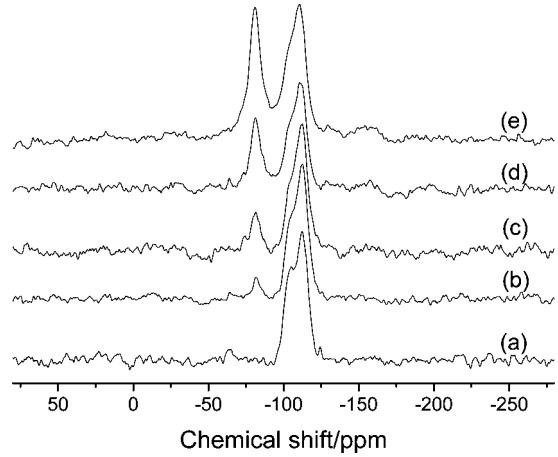

Figure 6. ^{29}Si MAS NMR spectra of (a) Co-HMS and CoPh-HMS-xx (where xx = (b) 10, (c) 20, (d) 30, and (e) 40).

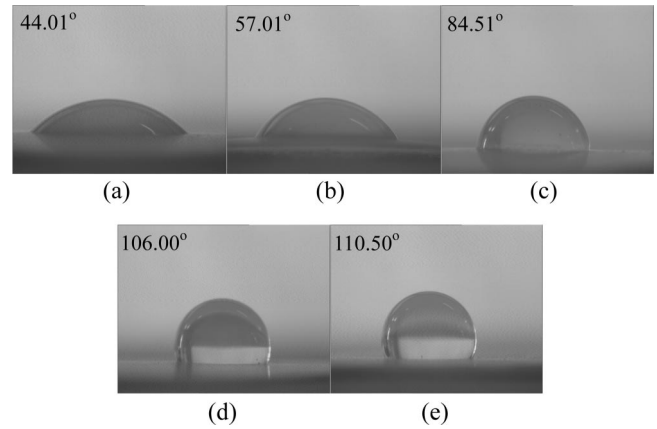

Figure 7. Images of sessile water droplets on the material flakes of (a) Co-HMS and CoPh-HMS-xx (where xx = (b) 10, (c) 20, (d) 30, and (e) 40).

materials, and this is consistent with the results of FT-IR spectroscopy.

With the immobilization of phenyl groups the surface of these bifunctionalized materials should have become more hydrophobic. To examine these changes the contact angles between sessile water droplets and the material flakes were measured. Figure 7 shows the images of water droplets on the material flakes. The numerical values of the contact angles were signed at the top left corner of the images. Without being organofunctionalized the surface of Co-HMS is hydrophilic with a water droplet contact angle of 44.01°. After being organofunctionalized the materials became more hydrophobic. The water droplet contact angles on the material flakes (CoPh-HMS-xx) increased with Ph-loading increase. The surface of CoPh-HMS-40 is the most hydrophobic with the largest water droplet contact angle of 110.50° in our work.

The catalytic performances of these materials were examined in the liquid-phase oxidation of cyclohexane with molecular oxygen as oxidant in the absence of solvent, and the results are

TABLE 2: Catalytic Oxidation of Cyclohexane over Different Catalysts[a]

		products distribution (%)[b]						
catalysts	conv. (%)	A	K	CHHP	acid	ester	K−A oil (%)	K/A ratio
Co-HMS	7.3	30.7	32.7	0.3	24.1	12.2	63.4	1.1
CoPh-HMS-10	8.0	28.8	43.1	0.2	19.0	8.9	71.8	1.5
CoPh-HMS-20	10.2	29.9	43.8	0.1	18.6	7.6	73.7	1.5
CoPh-HMS-30	9.3	30.8	43.0	0.2	18.9	7.1	73.8	1.4
CoPh-HMS-40	9.4	28.2	42.7	0.1	20.0	9.0	70.9	1.5

[a] Reaction was carried out with 0.12 g of catalyst and 0.12 g of TBHP in 15 g of cyclohexane at 393 K for 6 h under 1.0 MPa O_2. [b] A, cyclohexanol; K, cyclohexanone; acid, mainly adipic acid; ester, dicyclohexyl adipate, hexanolactone, and other ester.

listed in Table 2. According to our design idea immobilization of phenyl groups may facilitate conversion of cyclohexane while further inhibiting the transformations of K−A oil. In fact, it can be found that the anticipant results were successfully obtained. Without organic modification Co-HMS showed a lower activity and cyclohexane conversion was 7.3% with only 63.4% selectivity to K−A oil. In the distribution of the products the selectivity of acid and ester reached 24.1% and 12.2%, respectively. When the bifunctionalized CoPh-HMS-xx were used higher cyclohexane conversion and selectivity to K−A oil were obtained simultaneously, and a higher K/A ratio was also obtained. Though conversion only increased by 0.7% with CoPh-HMS-10 as catalyst, the selectivity of K−A oil increased by 8.4%. This result preliminarily exhibited the organic modification effect on the catalytic performance. CoPh-HMS-20 was found to be the best catalyst, and 10.2% conversion with 73.7% selectivity to K−A oil were obtained, which was higher than those obtained using metal-substituted AlPO-n or MCM-41 as catalyst.[3,31] Another noticeable phenomenon is that the selectivity of the ester monotonically decreased with an increase of Ph loading (≤30 mol %). As intented, hydrophobic phenyl groups were immobilized on the surface of CoPh-HMS-xx. Compared with the nonmodified Co-HMS, the surfaces of CoPh-HMS-xx have become more hydrophobic. On this more hydrophobic surface the almost nonpolar reactant cyclohexane is more easily adsorbed and the formed polar oxygenated products K−A oil (the dipolar moments of cyclohexanone and cyclohexanol are 2.87 and 1.86 D, respectively) can be desorbed more quickly. Thereby, conversion of cyclohexane was facilitated and further transformations of these primary products were inhibited. Moreover, the dipolar moment of adipic acid is 4.04 D, which is much higher than that of cyclohexane, cyclohexanone, or cyclohexanol. Compared with these three kinds of molecules adipic acid is more difficultly adsorbed onto the surface of the catalyst. Consequently, reaction of the acid with cyclohexanol was inhibited, resulting in the apparent decrease of the selectivity to ester. However, conversion of cyclohexane did not monotonically increase with Ph-loading increase. In fact, CoPh-HMS-30 and CoPh-HMS-40 showed lower activities than CoPh-HMS-20. One of the possible reasons may be attributed to the fact that with more phenyl groups immobilized the pore volume and surface area decreased greatly and the catalytically active centers may be sheltered by superabundant phenyl groups; thus, the activity was not further improved at higher Ph loading. In particular, with CoPh-HMS-40 being used, which has the poorest mesoporous structure in our work, the selectivity of K−A oil decreased apparently. A similar phenomenon was observed by Igarashi and co-workers.[32] As CoPh-HMS-20 was the most active catalyst, we chose this catalyst for more detailed study.

The effect of reaction temperature on conversion of cyclohexane and products distributions is shown in Figure 8. At 383 K, the lowest cyclohexane conversion (3.2%) and the highest

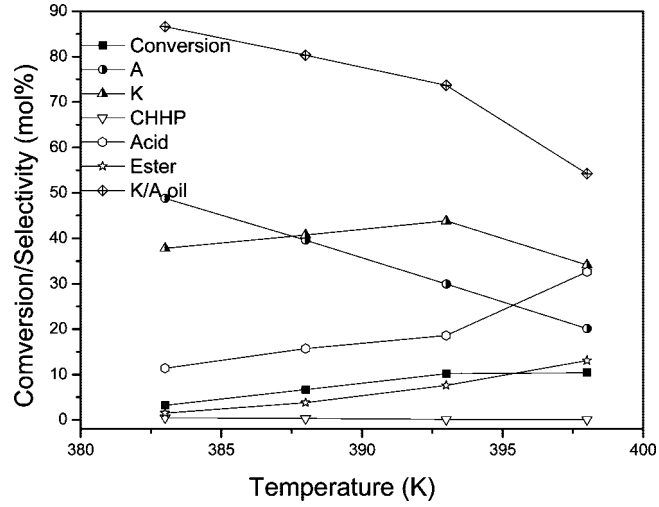

Figure 8. Influence of reaction temperature on CoPh-HMS-20 performance.

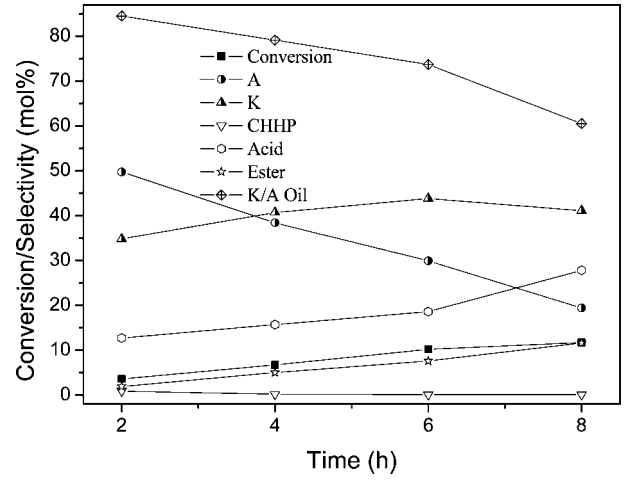

Figure 9. Influence of reaction time on CoPh-HMS-20 performance.

selectivity to K−A oil (86.6%) were obtained. With elevating temperature a gradual increase of cyclohexane conversion along with a decrease in the selectivity to K−A oil was observed, implying deep oxidation occurred at higher temperature. As a result the selectivity of acid increased remarkably. As in the change trend of acid, the selectivity of the ester increased with temperature too. Considering the effect of temperature on cyclohexane conversion and selectivity to K−A oil, the highest yield of K−A oil can be obtained at 393 K; this temperature was chosen as the suitable temperature for selective oxidation of cyclohexane.

Figure 9 shows the time dependence of product distributions in CoPh-HMS-20-catalyzed oxidation of cyclohexane at 393 K. At the initial 2 h a remarkable phenomenon different from

the further reaction was that the selectivity of CHHP reached nearly 1%. With increasing reaction time CHHP almost disappeared (≤0.3%). This shows that CHHP is an unstable intermediate and could decompose to cyclohexanone and cyclohexanol.[33] The selectivity of K−A oil decreased with further increasing reaction time. For each component of K−A oil the change trends of cyclohexanone and cyclohexanol were different. The selectivity of cyclohexanol decreased during the reaction period, while the selectivity of cyclohexanone increased at first and then decreased. At the same time, the selectivity of acid increased more apparently too. This indicates that cyclohexanol was continuously oxidized to cyclohexanone, which is in turn converted to acid. This was because both cyclohexanone and cyclohexanol are oxidized many times faster than cyclohexane itself.[33] Thus, for obtaining high selectivity to K−A oil the reaction time should not be too long.

Finally, in the recyclability test CoPh-HMS-20 was found to be stable and could be repeatedly used 3 times without activity decrease. In addition, similar to other works,[1,31,34] the observations that the free-radical initiator (TBHP) could increase both the rate and degree of conversion of cyclohexane while the free-radical scavenger (hydroquinone) could inhibit the reaction and CHHP existed only in the initial reaction stages (before 2 h) confirmed us that cyclohexane oxidation proceeded by a free-radical mechanism under these conditions.

4. Conclusion

A series of bifunctionalized material CoPh-HMS with different phenyl groups were successfully synthesized via a one-step co-condensation method. With these bifunctionalized materials as catalysts for cyclohexane oxidation the increase of cyclohexane conversion and selectivity to K−A oil along with the apparent decrease of selectivity to ester were achieved. An appropriate amount of phenyl group immobilization could make the material maintain good mesoporous structure and facilitate obtaining good activity. These results show that the combination of metal incorporation and organic modification methods is an effective design idea for cyclohexane oxidation. Considering that the selective oxidation reactions of hydrocarbon have one common characteristic, in which the substrates are weak polar molecules while the oxygenated products are stronger polar molecules, this design idea can also be utilized for other kinds of hydrocarbon-selective oxidations.

Acknowledgment. This work was supported by the National Natural Science Foundation of China (20603038, 20672111, and 20736010).

References and Notes

(1) Raja, R.; Sankar, G.; Thomas, J. M. *J. Am. Chem. Soc.* **1999**, *121*, 11926.

(2) Weissermel, K. Arpe, H. J. *Industrial Organic Chemistry*, 2nd ed.; VCH Press: Weinheim, 1993.

(3) Zhou, L.; Xu, J.; Miao, H.; Li, X.; Wang, F. *Catal. Lett.* **2005**, *99*, 231.

(4) Thomas, J. M.; Raja, R.; Sankar, G.; Bell, R. G. *Stud. Surf. Sci. Catal.* **2000**, *130*, 887.

(5) Schuchardt, U.; Cardoso, D.; Sercheli, R.; Pereira, R.; da Cruz, R. S.; Guerreiro, M. C.; Mandelli, D.; Spinacé, E. V.; Pires, E. L. *Appl. Catal., A* **2001**, *211*, 1.

(6) Tanev, P. T.; Pinnavaia, T. J. *Science* **1995**, *267*, 865.

(7) Tanev, P. T.; Pinnavaia, T. J. *Chem. Mater.* **1996**, *8*, 2068.

(8) Tanev, P. T.; Chibwe, M.; Pinnavaia, T. J. *Nature* **1994**, *368*, 321.

(9) Tuel, A.; Gontier, S.; Teissier, R. *Chem. Commun.* **1996**, *5*, 651.

(10) Zhang, W.; Wang, J.; Tanev, P. T.; Pinnavaia, T. J. *Chem. Commun.* **1996**, *8*, 979.

(11) Liu, H.; Lu, G.; Guo, Y.; Guo, Y.; Wang, J. *Nanotechnology* **2006**, *17*, 997.

(12) Bachari, K.; Cherifi, O. *J. Mol. Catal. A* **2006**, *253*, 187.

(13) Valkenberg, M. H.; Holderich, W. F. *Catal. Rev. Sci. Eng.* **2002**, *44*, 321.

(14) Mori, Y.; Pinnavaia, T. J. *Chem. Mater.* **2001**, *13*, 2173.

(15) Chen, C.; Zhou, L.; Zhang, Q.; Ma, H.; Miao, H.; Xu, J. *Nanotechnology* **2007**, *18*, 215603.

(16) Lim, M. H.; Stein, A. *Chem. Mater.* **1999**, *11*, 3285.

(17) Wahab, M. A.; Kim, I. I.; Ha, C. *Microporous Mesoporous Mater.* **2004**, *69*, 19.

(18) Williams, T.; Beltramini, J.; Lu, G. Q. *Microporous Mesoporous Mater.* **2006**, *88*, 91.

(19) Hamdy, M. S.; Ramanathan, A.; Maschmeyer, T.; Hanefeld, U.; Jansen, J. C. *Chem. Eur. J.* **2006**, *12*, 1782.

(20) Katsoulidis, A. P.; Petrakis, D. E.; Armatas, G. S.; Trikalitis, P. N.; Pomonis, P. J. *Microporous Mesoporous Mater.* **2006**, *92*, 71.

(21) Haskouri, J. E.; Cabrera, S.; Gomes-Garcia, C. J.; Guillem, C.; Latorre, J.; Beltran, A.; Beltran, D.; Marcos, M. D.; Amoros, P. *Chem. Mater.* **2004**, *16*, 2805.

(22) Carvalho, W. A.; Varaldo, P. B.; Wallau, M.; Schuchardt, U. *Zeolite* **1997**, *18*, 408.

(23) Karthik, M.; Tripathi, A. K.; Gupta, N. M.; Vinu, A.; Hartmann, M.; Palanichamy, M.; Murugesan, V. *Appl. Catal., A* **2004**, *268*, 139.

(24) Lambert, J. B.; Shurvell, H. F.; Lightner, D. A.; Cooks, R. G. *Introduction to Organic Spectroscopy*; Macmillan: New York, 1987; p 281.

(25) Alba, M. D.; Luan, Z. H.; Klinowski, J. *J. Phys. Chem.* **1996**, *100*, 2178.

(26) Carrado, K. A.; Xu, L.; Csencsits, R.; Muntean, J. V. *Chem. Mater.* **2001**, *13*, 3766.

(27) Gallo, J. M. R.; Pastore, H. O.; Schuchardt, U. *J. Catal.* **2006**, *243*, 57.

(28) *Materials Research Society Symposium Proceedings*; Schwarz, S., Corbin, D. R., Vega, A. J., Lobo, R. F., Beck, J. S., Suib, S. L., Corbin, D. R., Davis, M. E., Iton, L. E., Zones, S. I., Eds.; Materials Research Society: Pittsburg, PA, 1996; Vol. 431, p 137.

(29) Engelhardt, G.; Jancke, H. *Polym. Bull.* **1981**, *5*, 577.

(30) Mercier, L.; Pinnavaia, T. J. *Chem. Mater.* **2000**, *12*, 188.

(31) Chen, J. O.; Sheldon, R. A. *J. Catal.* **1995**, *153*, 1.

(32) Igarashi, N.; Kidani, S.; Ahemaito, R.; Hashimoto, K.; Tatsumi, T. *Microporous Mesoporous Mater.* **2005**, *81*, 97.

(33) Suresh, A. K.; Sharma, M. M.; Sridhar, T. *Ind. Eng. Chem. Res.* **2000**, *39*, 3958.

(34) Zhou, L.; Xu, J.; Miao, H.; Wang, F.; Li, X. *Appl. Catal., A* **2005**, *292*, 223.

JP809427T